Published in final edited form as:

J Am Chem Soc. 2018 February 14; 140(6): 2020–2023. doi:10.1021/jacs.7b12766.

Photoactivatable Sensors for Detecting Mobile Zinc

Jacob M. Goldberg[†,§], **Fang Wang**[†,§], **Chanan D. Sessler**[†], **Nathan W. Vogler**[‡], **Daniel Y. Zhang**[†], **William H. Loucks**[†], **Thanos Tzounopoulos**[‡], and **Stephen J. Lippard**[*,†]

[†]Department of Chemistry, Massachusetts Institute of Technology, 77 Massachusetts Avenue, Cambridge, Massachusetts 02139, United States

[‡]Pittsburgh Hearing Research Center, Department of Otolaryngology, University of Pittsburgh, 3501 Fifth Avenue, Pittsburgh, Pennsylvania 15261, United States

Abstract

Fluorescent sensors for mobile zinc have proven valuable for studying complex biological systems. Because these sensors typically bind zinc rapidly and tightly, there has been little temporal control over the activity of the probe after its application to a sample. The ability to control the activity of a zinc sensor in vivo during imaging experiments would greatly improve the time resolution of the measurement. Here, we describe photoactivatable zinc sensors that can be triggered with short pulses of UV light. These probes are prepared by functionalizing a zinc sensor with protecting groups that render the probe insensitive to metal ions. Photo-induced removal of the protecting groups restores the binding site, allowing for zinc-responsive changes in fluorescence that can be observed in live cells and tissues.

Zinc is an essential element for human health. Throughout the body, zinc is found tightly bound to proteins either as a catalytic cofactor or structural element.[1] In some tissues, particularly those of the brain, pancreas, prostate, and mammary gland, zinc exists in ion pools that participate in signaling cascades and regulatory networks.[2] This so-called mobile zinc acts as a brake to attenuate glutamatergic neurotransmission in certain areas of the brain engaged in sensory perception, especially in auditory processing,[3–5] and also as a signaling agent in fertilization.[6] Despite much research, the exact functional role of mobile zinc in these pathways is not completely understood. A critical barrier to understanding the role of mobile zinc is a lack of suitable probes for studying these systems with high spatiotemporal resolution.[7]

Many probes are described in the literature, some of which have been used to great advantage to study the role of zinc in biological processes.[8] Probes that fluoresce exclusively in the presence of zinc are among the most common and can be categorized as those derived from small molecule and protein-based fluorophores. These sensors employ diverse

[*]**Corresponding Author:** lippard@mit.edu.

[§]**Author Contributions**: These authors contributed equally.

Supporting Information. This material is available free of charge via the Internet at http://pubs.acs.org. Experimental methods, computational details, and characterization data (PDF).

Notes

The authors declare no competing financial interest.

mechanisms for detecting zinc in biological systems, ranging from changes in photoinduced electron transfer or Förster resonance energy transfer to complete structural rearrangements that occur upon zinc binding.[8–11] In almost all cases, the sensors respond to zinc rapidly.

Generally, a fast zinc response is an advantageous property because many zinc-signaling events, such as synaptic zinc release, occur on short timescales. Nonetheless, there are certain circumstances in which such a fast zinc response can be problematic. Consider the case of Zinpyr-1 (ZP1).[12] In cells with low cytosolic zinc concentrations, such as HeLa, ZP1 localizes to the Golgi apparatus, where it can then detect exogenously added zinc. If cells have high concentrations of cytosolic zinc, the probe can be saturated with the ion before it reaches the Golgi. For cells that secrete zinc or samples that need to be maintained in zinc-rich media, the sensor can be completely saturated with extracellular zinc before it even crosses the cell membrane. These features are not specific to ZP1 and limit the utility of many small molecule metal ion sensors, particularly those used in applications for which it is essential that the sensor be delivered to a programed location without detecting an analyte during transit.

To overcome these challenges, we devised a sensor that would not respond to zinc until it is selectively activated in a biological sample. In this manner, the sensor could be delivered to any site of interest in a cell or tissue sample without detecting zinc ions encountered in transit. Upon reaching the desired target, the construct could be selectively and quickly activated to reveal a fast and tight binding zinc probe. With these goals in mind, we designed a series of protected zinc sensors based on the ZP1 scaffold that met all requirements. We chose photocleavable protecting groups, which are widely used in biological experiments because they can be readily removed with short pulses of light and provide excellent spatial and temporal control over the release of caged molecules including fluorescein.[13] This strategy has proved effective for copper sensing.[14] A similar approach has been used for preparing caged DNAzymes that sense metal ions, including zinc and lead, but this method requires treating cells with a DNAzyme and transfection reagents for several hours prior to imaging, which may not be suitable for all applications.[15]

As shown in Scheme 1, our strategy requires masking the ZP1 xanthene-ring oxygen atoms involved in zinc binding by functionalizing them with bulky *O*-Nitrobenzyl groups. This modification forces the fluorescein scaffold to adopt a non-fluorescent lactone form and, as supported by theoretical calculations, disrupts the zinc-binding site (see Supporting Information). Upon irradiation of the protected molecule with ultraviolet light, ZP1 is released and exhibits its typical zinc-sensing behavior.

We prepared four ZP1 derivatives (**1**–**4**) by modifying a published fluorescein diether synthesis[16] because direct dialkylation of ZP1 did not give the desired regioisomer (Scheme S3). For each sensor, we measured the absorbance and fluorescence in the presence and absence of excess zinc before and after irradiation at 254 or 380 nm, and we followed the course of each reaction by HPLC (Figures S5–S20). In these studies, **1**, **2**, and **3** were photoactivatable as anticipated, but **4** was not. Representative results are shown in Figure 1. The protected sensor **3** was not fluorescent in the absence of zinc. Essentially no increase in fluorescence was observed from the same solution when $ZnCl_2$ was added. The fluorescence

then increased considerably upon UV-irradiation, consistent with removal of the protecting groups and restoration of the fluorophore. Finally, addition of the zinc chelator tris(2-Pyridylmethyl)amine (TPA)[17] to the samples reduced the fluorescence. HPLC analysis of the cuvette solutions confirmed that ZP1 was generated after irradiation with UV light. Similar results were obtained for sensors **1** and **2**. In contrast, irradiation of the sensors in the absence of zinc induced only modest increases in fluorescence. Only trace amounts of ZP1 were detected by HPLC analysis under these conditions. As expected, the fluorescence intensity did not increase significantly upon addition of $ZnCl_2$. Sensor **4** did not exhibit a satisfactory response in any of the tested conditions. Although sensor **2** was rapidly photoactivated in the presence of zinc, irradiation of the sensor in the absence of zinc also elicited a substantial increase in fluorescence, which could lead to false positive results in biological experiments. Such concerns prompted us to exclude sensors **2** and **4** in further studies. In these and separate experiments, we observed that all sensors—including ZP1—decompose during extended periods of irradiation with UV light, particularly in the absence of zinc, and therefore sensors that can be activated rapidly and specifically are especially advantageous. Sensors **1** and **3** meet these requirements.

We conducted a variety of experiments to find robust and reproducible imaging methods. Because the protected sensors are not fluorescent, calculated fluorescence turn-on values (F/F_0) were extremely sensitive to small variations in initial fluorescence (F_0), including those that arise from inadvertent activation of the sensor in trace amounts by stray light. It is therefore important to conduct imaging procedures in the dark. In a typical experiment, HeLa cells were incubated with the sensor to be tested in dye-free, serum-free medium (DMEM) with a small amount of Pluronic F-127, a nonionic surfactant.[18] After 15 min, the medium was removed and the cells were washed thoroughly with phosphate-buffered saline (PBS). Fresh dye-free, serum-free DMEM was added to the culture dishes and the cells were imaged immediately. Zinc pyrithione (ZnPT) was added to the cells on the microscope stage and, after several minutes, additional images of the same cells were acquired for comparison. Representative images for sensor **3** are shown in Figure 2. The sensor was essentially non-fluorescent in cells, even in the presence of high concentrations of zinc. Irradiation for 15 s on the microscope stage using a standard DAPI filter set was sufficient to activate the sensors with an average integrated fluorescence turn-on of 19 ± 1. Addition of TPA led to an approximately 60% reduction in fluorescence, a result typically observed for ZP1 in cells.[17] Sensor **1** gave qualitatively similar results in analogous experiments (Figure S25).

Cells treated with **3** in the absence of any added zinc exhibited an approximately 5-fold increase in fluorescence after irradiation. Addition of ZnPT produced an additional 25% increase in fluorescence intensity that could be reversed by addition of TPA. Although similar results were obtained with sensor **1**, we observed that irradiation of **1** in the absence of exogenous zinc induced a stronger fluorescence response in cells, on average, than irradiation of **3** (Figures S23–24). Moreover, the higher sensitivity of **1** to UV light relative to that of **3** may lead to inadvertent activation by stray light. For these reasons, we restricted subsequent studies to **3**.

We were especially interested in testing **3** in systems in which typical small molecule sensors, such as ZP1, tend to have difficulty—specifically (A) under conditions in which cells must be maintained in zinc-rich medium or (B) when cells have high cytosolic concentrations of mobile zinc. To mimic condition A, we spiked the culture medium with $ZnCl_2$ before adding the sensors. ZP1 does not show appreciable cell permeability under these conditions and addition of ZnPT did not trigger an increase in fluorescence (Figure S29). Under similar conditions, **3** appears to cross the cell membrane readily. Irradiation of the cells after addition of ZnPT induced an approximately 50-fold increase in fluorescence that could be reduced by treatment with TPA (Figure S26). In the absence of ZnPT, the fluorescence increased by only 7.5-fold upon irradiation (Figure S28).

In separate experiments, HeLa cells were treated with ZnPT and then washed before addition of any sensor to test condition B. Unlike when ZnPT is added to cells pre-treated with ZP1 and induces a fluorescence response localized to the Golgi apparatus, in these experiments bright fluorescence was observed throughout the entire cell body (Figure S30). Irradiation of cells treated with **3** under these conditions, however, revealed distinct, characteristic patterns of localized fluorescence (Figure S27). These results confirm that **3** is a superior sensor for imaging cells that must be maintained in zinc-rich environments.

To evaluate our ability to control activation of the sensor with high spatiotemporal resolution, we tested **3** in live brain slices. For this work, we examined the murine dorsal cochlear nucleus (DCN), a region of the brain that integrates signals from auditory nerve inputs in the vesicular zinc-lacking deep layer with information arriving from other areas of the brain in the vesicular zinc-rich molecular layer (Figure 3).[3–4, 19–21] Because the zinc-lacking and zinc-rich lacking layers are anatomically well-defined, the DCN is ideal for testing photoactivation of the sensor. Acute DCN slices incubated with **3** were irradiated with 355 nm laser light in a square grid pattern spanning both the zinc-rich molecular layer and the zinc-deficient deep layer. As shown in Figure 3, after 5 ms of irradiation, only sites in the molecular layer exhibited significant increases in fluorescence intensity after photostimulation, while sites in the deep layer did not. Importantly, the fluorescence response was restricted to loci of direct excitation; fluorescence signals from tissue between or outside those regions were not affected. In contrast, the diacetylated derivative of ZP1 fluoresces brightly in the entire molecular layer.[4] This proof-of-principle experiment shows that **3** can be selectively activated in live tissue slices with at least micrometer spatial resolution and millisecond temporal resolution.

In conclusion, we synthesized photoactivatable zinc sensors based on the ZP1 scaffold that can be used to image zinc in cells and tissue with high spatiotemporal resolution. Because the properties of the ZP1 family can easily be tuned synthetically, we expect that the strategy presented here can be used to prepare photoactivatable sensors with nanomolar to millimolar zinc-binding affinities. Furthermore, we envision this method to be generally applicable to the protection of fluorescein-based sensors for other analytes, including copper, iron, and nitric oxide.[22–25]

Supplementary Material

Refer to Web version on PubMed Central for supplementary material.

Acknowledgments

This work was supported by funding from National Institutes of Health grants R01-GM065519 (to S.J.L.) and R01-DC007905 (to T.T.) and fellowships F32-GM109516 (to J.M.G.) and F31-DC015924 (to N.W.V.). D.Y.Z and W.H.L. thank the MIT Undergraduate Research Opportunities Program for support. The Massachusetts Green High Performance Computing Center is acknowledged for providing computational resources.

References

1. Maret W. Adv Nutr. 2013; 4:82–91. [PubMed: 23319127]
2. Hennigar SR, Kelleher SL. Biol Chem. 2012; 393:565–578. [PubMed: 22944660]
3. Anderson CT, Radford RJ, Zastrow ML, Zhang DY, Apfel U-P, Lippard SJ, Tzounopoulos T. Proc Natl Acad Sci USA. 2015; 112:E2705–E2714. [PubMed: 25947151]
4. Kalappa BI, Anderson CT, Goldberg JM, Lippard SJ, Tzounopoulos T. Proc Natl Acad Sci USA. 2015; 112:15749–15754. [PubMed: 26647187]
5. Anderson CT, Kumar M, Xiong S, Tzounopoulos T. eLife. 2017; 6:e29893. [PubMed: 28887876]
6. Que EL, Bleher R, Duncan FE, Kong BY, Gleber SC, Vogt S, Chen S, Garwin SA, Bayer AR, Dravid VP, Woodruff TK, O'Halloran TV. Nat Chem. 2015; 7:130–139. [PubMed: 25615666]
7. Barr CA, Burdette SC. Essays Biochem. 2017; 61:225–235. [PubMed: 28487399]
8. Carter KP, Young AM, Palmer AE. Chem Rev. 2014; 114:4564–4601. [PubMed: 24588137]
9. Hessels AM, Merkx M. Metallomics. 2015; 7:258–266. [PubMed: 25156481]
10. McRae R, Bagchi P, Sumalekshmy S, Fahrni CJ. Chem Rev. 2009; 109:4780–4827. [PubMed: 19772288]
11. Que EL, Domaille DW, Chang CJ. Chem Rev. 2008; 108:1517–1549. [PubMed: 18426241]
12. Walkup GK, Burdette SC, Lippard SJ, Tsien RY. J Am Chem Soc. 2000; 122:5644–5645.
13. Klán P, Šolomek T, Bochet CG, Blanc A, Givens R, Rubina M, Popik V, Kostikov A, Wirz J. Chem Rev. 2013; 113:119–191. [PubMed: 23256727]
14. Yuan L, Lin W, Cao Z, Long L, Song J. Chem - Eur J. 2011; 17:689–696. [PubMed: 21207590]
15. Hwang K, Wu P, Kim T, Lei L, Tian S, Wang Y, Lu Y. Angew Chem Int Ed. 2014; 53:13798–13802.
16. Wysocki LM, Grimm JB, Tkachuk AN, Brown TA, Betzig E, Lavis LD. Angew Chem Int Ed. 2011; 50:11206–11209.
17. Huang Z, Zhang X-a, Bosch M, Smith SJ, Lippard SJ. Metallomics. 2013; 5:648–655. [PubMed: 23715510]
18. Poenie M, Alderton J, Steinhardt R, Tsien R. Science. 1986; 233:886–889. [PubMed: 3755550]
19. Frederickson CJ, Howell GA, Haigh MD, Danscher G. Hear Res. 1988; 36:203–211. [PubMed: 3209493]
20. Rubio ME, Juiz JM. J Comp Neurol. 1998; 399:341–358. [PubMed: 9733082]
21. Oertel D, Young ED. Trends Neurosci. 2004; 27:104–110. [PubMed: 15102490]
22. Izumi S, Urano Y, Hanaoka K, Terai T, Nagano T. J Am Chem Soc. 2009; 131:10189–10200. [PubMed: 19572714]
23. Thomas F, Serratrice G, Béguin C, Aman ES, Pierre JL, Fontecave M, Laulhère JP. J Biol Chem. 1999; 274:13375–13383. [PubMed: 10224100]
24. Aron AT, Loehr MO, Bogena J, Chang CJ. J Am Chem Soc. 2016; 138:14338–14346. [PubMed: 27768321]
25. Kuhn MA, Hoyland B, Carter S, Zhang C, Haugland RP. Proc SPIE. 1995; 2388:238–244.

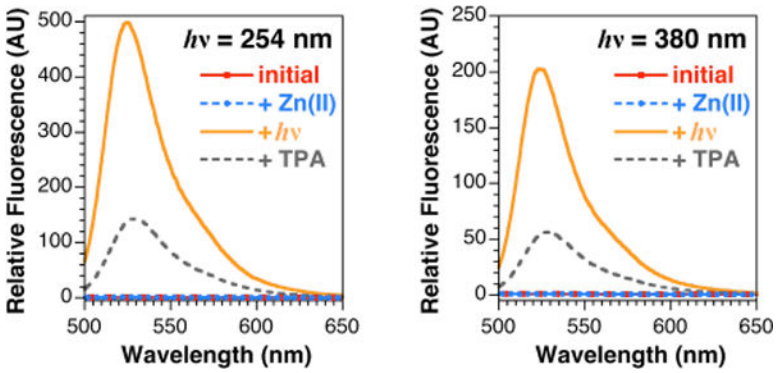

Figure 1.

Emission spectra of 3 μM **3** in 5 mM PIPES, 10 mM KCl in 30% CH_3CN in H_2O (v/v), pH 7.0 at 298 K; in the presence of 10 μM $ZnCl_2$; after irradiation for 240 s with 254 nm (left) or 380 nm (right) light; and after addition of 20 μM tris(2-pyridylmethyl)amine (TPA).

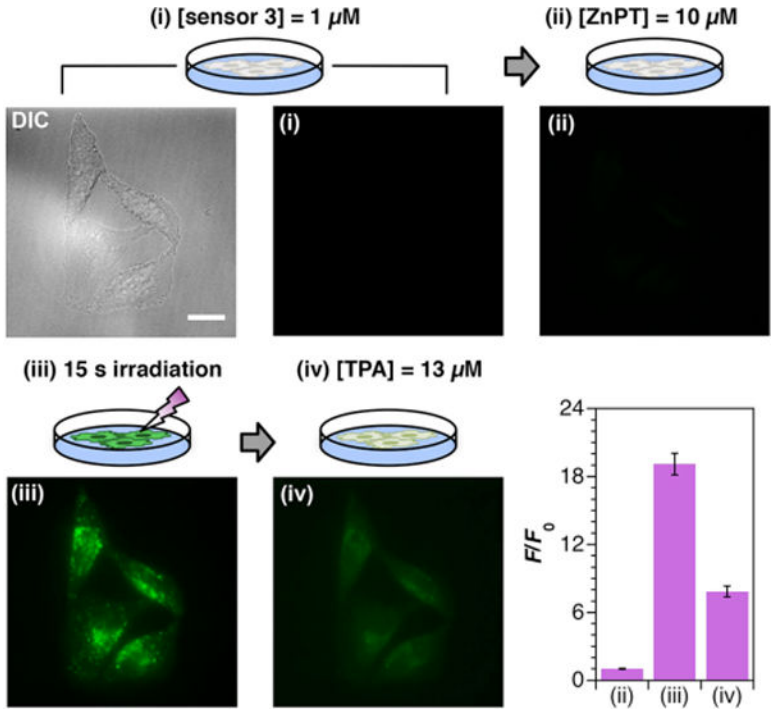

Figure 2.

Differential interference contrast (DIC) and fluorescence microscopy images of (i) HeLa cells treated with 1 μM **3**; (ii) after treatment with 10 μM zinc pyrithione (ZnPT); (iii) after UV irradiation for 15 s with a DAPI filter set; and (iv) after subsequent incubation with 13 μM TPA. The average integrated fluorescence turn-on is shown with standard error ($n = 82$). All p-values $<10^{-20}$. Scale bar = 25 μm.

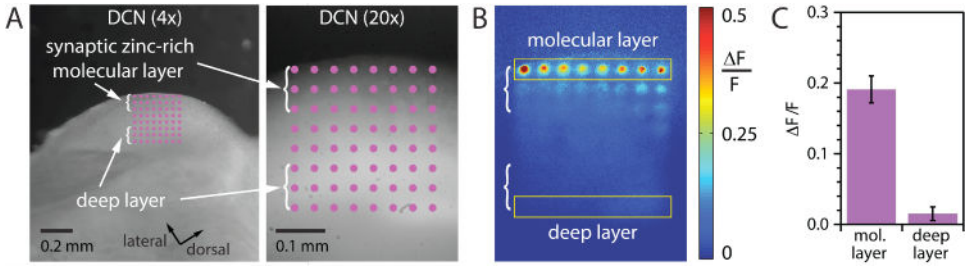

Figure 3.

Fluorescence of **3** in brain slices containing the dorsal cochlear nucleus (DCN) after photoactivation. (A) 4× image of the DCN slice (left), with overlaid 8 × 8 photostimulation grid (40 μm spacing). 20× image of the DCN (right) with the overlaid grid. The grid was photostimulated 5 times with 1 ms pulses (355 nm, ~5.5 mW). (B) Heat map of normalized fluorescent signals. $\Delta F/F$ is the fluorescence change after photostimulation divided by the initial fluorescence. (C) Comparison of the average photoactivated fluorescence of sensor **3** in the molecular layer versus the deep layer (regions outlined by yellow boxes in B, $n = 6$, $p < 0.0001$, unpaired t test).

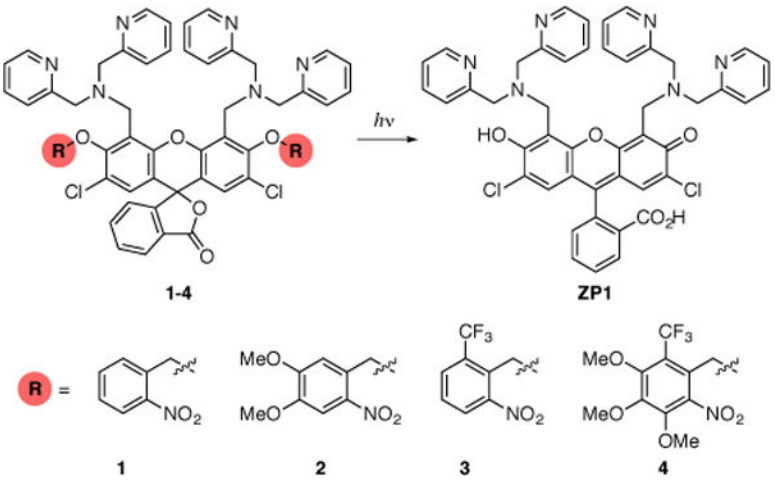

Scheme 1.

Removal of Photocleavable Protecting Groups from ZP1 to Give an Active Sensor.